Available online at www.sciencedirect.com
SCIENCE DIRECT
Polymer Degradation and Stability 86 (2004) 171–178
Polymer Degradation and Stability
www.elsevier.com/locate/polydegstab

Thermal degradation of poly(acrylic acid) containing copper nitrate

Stanislav Dubinsky[a], Gideon S. Grader[b], Gennady E. Shter[b], Michael S. Silverstein[a,*]

[a]Department of Materials Engineering, Technion—Israel Institute of Technology, Haifa 32000, Israel
[b]Department of Chemical Engineering, Technion—Israel Institute of Technology, Haifa 32000, Israel

Received 29 January 2004; received in revised form 9 April 2004; accepted 10 April 2004

Abstract

A high temperature superconductor (HTSC) precursor containing a polymer and metal nitrates may be processed with relative ease before pyrolysis. This article focuses on the thermal decomposition of poly(acrylic acid) (PAAc) containing copper nitrate (Cu–N) as a first step in the study of an HTSC precursor containing copper, barium and yttrium nitrates. The degradation of PAAc/Cu–N was found to be a complex multi-stage process that was not always directly related to the degradation of the individual components. Adding Cu–N to PAAc causes a dramatic decrease in thermal stability. While the degradation of PAAc in argon yields a carbonaceous residue, no such residue was found for the degradation of PAAc/Cu–N in air. The rate of PAAc/Cu–N degradation is significantly higher in air than in argon. The decomposition mechanisms include polymer chain scission catalysed by copper ions and the formation of terminal macroradicals that generate low molecular weight organic compounds.

Keywords: Degradation; Poly(acrylic acid); Pyrolysis; Copper nitrate; Thermogravimetric analysis (TGA)

1. Introduction

A novel way to prepare high temperature superconductor (HTSC) ceramic films and fibres involves the use of precursors containing polymer–metal complexes [1–12]. For example, films cast from a solution containing a polymer and Y, Ba and Cu nitrates can be pyrolyzed to form the $YBa_2Cu_3O_{7-x}$ (YBCO) HTSC [1]. Polymers that have been investigated for such HTSC precursors include poly(methacrylic acid) [2–6], novolac [1,3,4,7,8], poly(*N*,*N*-dicarboxymethyl)allylamine [9], polyacrylonitrile (PAN) [10], and copolymers of acrylic acid and acrylamide [11]. An HTSC precursor based on a UV-sensitive polymer can be patterned using photolithography to form such structures as microbridges prior to pyrolysis [1,3–7,12].

The presence of metal nitrate salts in a PAN-based HTSC precursor has been shown to significantly affect polymer degradation [10,13]. The degradation of an HTSC precursor based on poly(acrylic acid) (PAAc) has not been investigated in detail. PAAc salts of Fe(III), Cr(III), Ni(II), Co(II), and Mn(II) have lower decomposition temperatures than PAAc, with the PAAc salts containing divalent metals being more stable than those containing trivalent metals [14]. The decomposition of PAAc salts in air generally yields metal oxides [14,15]. The decomposition of PAAc salts in argon or nitrogen can also produce metals and carbonaceous residue [14,16,17]. The degradation of PAAc salts has been described in terms of both main chain and side group scission reactions involving the formation of alkenes, cyclic ketones and ketenes, aldehydes, methane and aromatics [18,19].

This article focuses on the thermal decomposition of PAAc containing copper nitrate (Cu–N), both in argon and in air. This study is the first step in the investigation of an HTSC precursor containing PAAc and copper, barium

* Corresponding author. Tel./fax: +972-4-829-4582.
E-mail address: michaels@tx.technion.ac.il (M.S. Silverstein).

0141-3910/$ - see front matter © 2004 Elsevier Ltd. All rights reserved.
doi:10.1016/j.polymdegradstab.2004.04.009

and yttrium nitrates. The focus on Cu–N reflects its ability to dominate the degradation process in HTSC precursors [10,13]. The use of both thermal analysis with simultaneous mass spectroscopy and FTIR analysis can yield a thorough understanding of the degradation mechanisms. Understanding the degradation process is an essential part of optimising the pyrolysis conditions for the production of the HTSC phase.

2. Experimental

2.1. Materials

The polymer used was a commercial PAAc with an average M_v of about 450,000 (Aldrich Chemical Company). Cu–N is copper (II) nitrate 2.5 hydrate [$Cu(NO_3)_2 \cdot 2.5H_2O$] (Riedel-de Haën). PAAc and Cu–N were used as received.

2.2. Sample preparation

The PAAc/Cu–N films were prepared as follows: 6 wt.% aqueous solutions of PAAc were prepared by stirring and heating in a water bath at 70 °C; Cu–N was added to the polymer solutions at different PAAc/Cu–N weight ratios: 10/1, 4/1, 2/1 (the materials will be referred to as '10/1', '4/1' and '2/1'); the solutions were cast on Teflon plates, heated at 60 °C in a circulating air oven for 24 h and then dried at 25 °C in vacuum. Powders were obtained by grinding the films using a mortar and pestle and then drying in a vacuum oven at 60 °C for 24 h.

2.3. Characterization

Differential scanning calorimetry (DSC) was carried out from 25 to 450 °C at 5 °C/min in either argon or dry air (4 ml/min) (Mettler DSC-821 calorimeter). The DSC samples were dry powders (4–6 mg) in an open aluminium pan and an empty aluminium pan was used as the reference. The DSC was also used to expose the materials to high temperatures prior to Fourier transform infrared spectroscopy (FTIR) characterization. The samples were heated in the DSC cell to the desired temperature at 5 °C/min and then quickly cooled to room temperature. The annealed samples were then characterized by FTIR to observe the changes in molecular structure. FTIR spectra from 500 to 4000 cm^{-1} at a resolution of 2 cm^{-1} were taken in transmittance using as-cast films or KBr pellets containing 1% of the sample by weight (Bruker Equinox 55).

Simultaneous thermogravimetric analysis (TGA) and differential thermal analysis (DTA) in situ with TGA were made from 25 to 1000 °C at 5 °C/min in either argon or air using 25 mg samples (Setaram 92-16.18 TGA). The differential thermal gravimetry (DTG) thermograms were derived from the TGA results using the supplied software. An analysis of the pyrolytic exhaust gases was conducted using an on-line quadrupole mass-spectrometer (Thermostar 200, Balzers Co.) synchronized with the TGA/DTA instrument.

3. Results and discussion

3.1. Degradation of Cu–N

The TGA, DTG, DTA and exhaust gas mass spectroscopy for Cu–N in argon and in air were performed to provide reference information. The pyrolysis of Cu–N included two main stages, dehydration and denitration, and proceeded much more rapidly in air. The residual mass of about 33.6% corresponded to the residual mass of 34.2% calculated for the pyrolysis of Cu–N to CuO. The degradation of Cu–N and the formation of CuO are described in more detail in the literature [20–22]. One exceptional observation made during pyrolysis in Ar (but not during pyrolysis in air) was the release of significant amounts of oxygen and of a gas with $m/z = 44$, most likely CO_2, between 800 and 900 °C. The origin of O_2 and CO_2 may lie in traces of carbon-containing contaminants seen in the FTIR spectrum of Cu–N [13] which can result in the formation of compounds such as carbonates.

3.2. Degradation of PAAc

The FTIR spectrum of PAAc at room temperature (Fig. 1a) has a prominent band at 1709 cm^{-1} associated with C=O stretching. In addition, there is a very broad OH stretching band at 3000 cm^{-1} superimposed on the CH, CH_2 stretching bands at 3100–2800 cm^{-1}. There are distinctive shoulders between 2700 and 2500 cm^{-1} from overtones and combinations of the C–O stretch band at 1200–1315 cm^{-1} and from in-plane deformation of C–O–H at 1450–1395 cm^{-1}. The wide band at 798 cm^{-1} is associated with an out-of-plane OH···O deformation indicating the existence of strong interchain hydrogen bonds [23]. These band assignments are summarized in Table 1 and are used for all the PAAc spectra.

The TGA, DTG, DTA and exhaust gas mass spectroscopy (MS) for PAAc in argon are found in Fig. 2. These data are summarized in Table 2, in which the behaviour of PAAc when heated in argon is divided into three main stages based on the DTA, DTG and MS peaks. The first stage (70–142 °C) is accompanied by a 2.5% mass loss, largely associated with the release of water (Fig. 2). The carboxyl group band undergoes a slight shift (from 1709 cm^{-1} to 1715 cm^{-1}), a slight broadening, and a significant decrease in its intensity relative to the other bands (Fig. 1b). These changes in

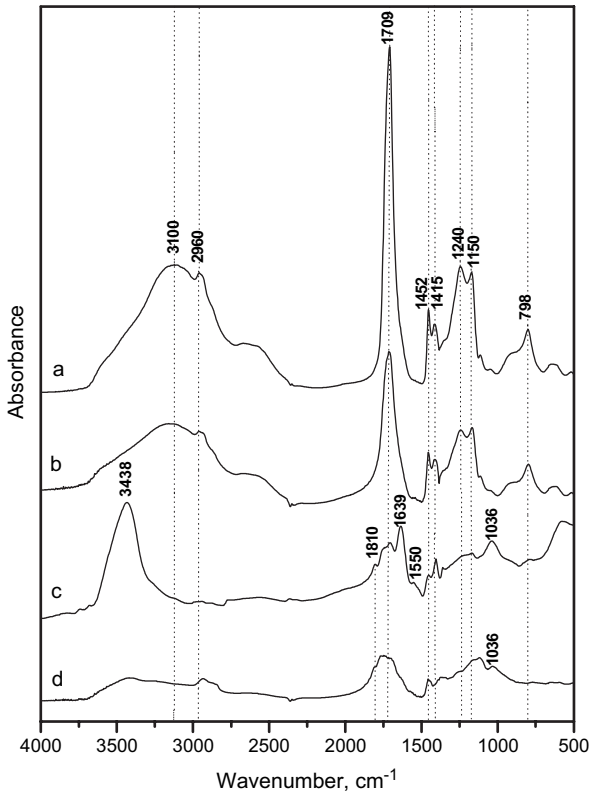

Fig. 1. FTIR spectra of PAAc after exposure to high temperatures in argon: (a) as cast; (b) 150 °C; (c) 240 °C; (d) 340 °C.

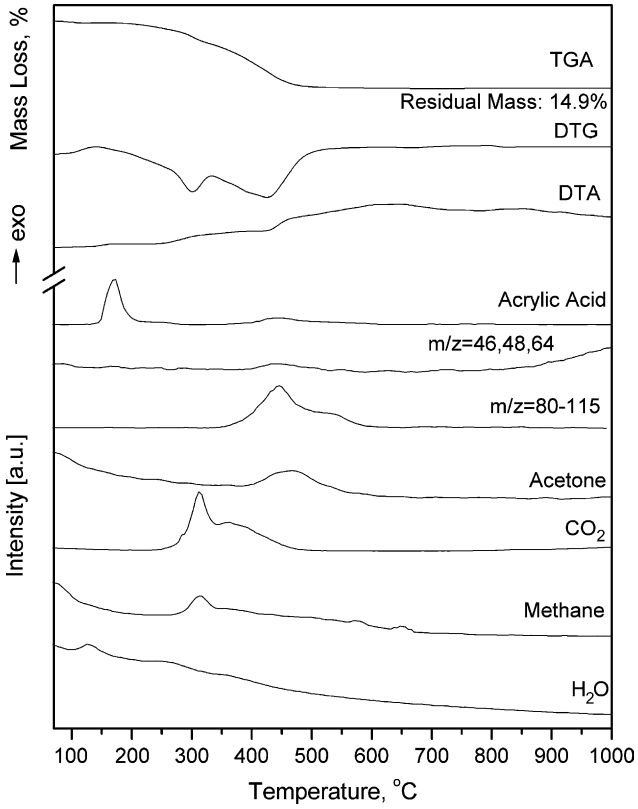

Fig. 2. Thermal analysis and exhaust mass spectra for PAAc in argon.

the carboxyl group indicate that anhydride-like structures have been formed [24]. Towards the end of the first stage, the PAAc is above its glass transition temperature (T_g) of 128 °C (from the DSC results). Above the T_g the mobility of the PAAc increases and residual acrylic acid monomer is released (Fig. 2).

The second stage (142–335 °C) is characterized by an endotherm of 0.42 kJ/g at 238 °C and a mass loss of 27.4% from the release of H_2O, CH_4 and acrylic acid monomer. The release of carbon dioxide (Fig. 2) reflects the decarboxylation of the anhydride structures and the formation of intermediate species, which then form ketenes, ketones and unsaturated compounds [25].

The FTIR spectrum of PAAc exposed to 240 °C in argon (Fig. 1c) is considerably different than that for the as-cast PAAc. The pronounced carboxylic group band at 1709 cm^{-1} in the as-cast material has split into four sharp peaks in the material exposed to 240 °C. The peaks at 1810 and 1751 cm^{-1} are related to glutaric anhydride [24]. The peak at 1036 cm^{-1} also indicates the presence of a non-conjugated cyclic anhydride [23]. The peak at 1705 cm^{-1} reflects carboxylic acid groups in the chains. The peak at 1639 cm^{-1} reflects unsaturated groups [23]. The vinyl CH_2 scissors deformation also gives rise to a medium intensity band at 1415 cm^{-1}. The relative height of the band at 1452 cm^{-1} reflecting C–O–H in-plane deformation is significantly smaller

Table 1
FTIR band assignments for PAAc and PAAc/Cu–N spectra

Group	PAAc (cm^{-1})	PAAc/Cu–N (cm^{-1})
OH–O out-of-plane deformation	798	–
Ketone	1150	1175
C–O stretch	1200–1315	1169, 1240
NO_3^- stretch	–	1385
COH in-plane deformation	1395–1450	–
C=C stretch	1639	1414, 1675
COO^- stretch	–	1640
COOH stretch	1709	1722
C–O–C (anhydride) stretch	1757, 1810	1740, 1760, 1802
CH, CH_2 stretch	2800–3100	2800–3100
OH stretch	3000	3435

Table 2
Summary of thermal analysis for PAAc in argon

Stage	TGA and DTG			DTA peaks (°C)	DSC heat (J/g)
	Onset (°C)	DTG peak (°C)	Mass loss (%)		
1	70	–	2.5	–	–
2	142	301	27.4	238, endo	417
3	335	425	55.2	337, endo	40
Total			85.1		

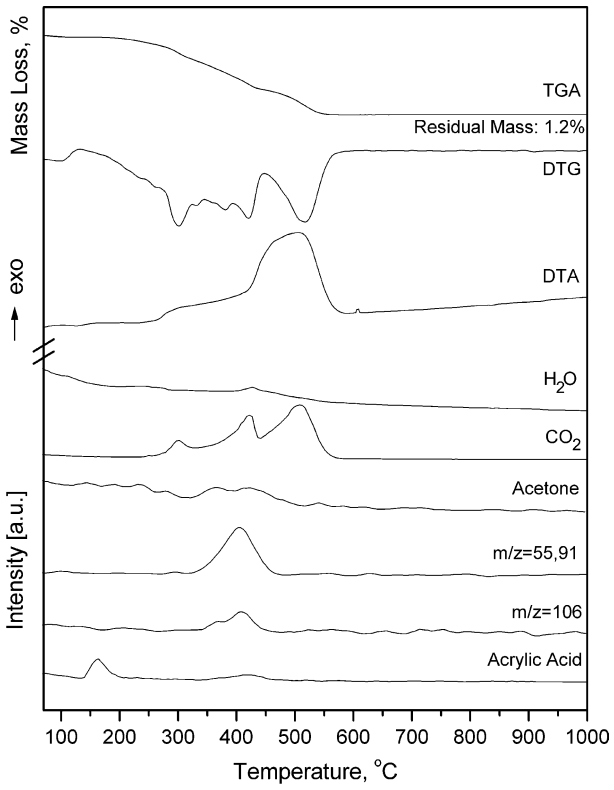

Fig. 3. Thermal analysis and exhaust mass spectra for PAAc in air.

indicating that there has been a considerable reduction in the amount of COH groups during anhydride formation. The absorption at 1150 cm^{-1} most likely indicates the presence of cyclic ketones [24]. The peak at 3438 cm^{-1} is associated with unbound OH groups and carbonyl group overtones [23].

The third stage of PAAc degradation in argon (from 335 °C) is characterized by a mass loss of 55.2% which is largely higher molecular weight species (Fig. 2). These species, with m/z from 46 to 115, are short chain fragments created by chain scission [25]. The release of acrylic acid moieties (Fig. 2) represents such a depolymerisation reaction [26]. The residual mass of carbonaceous residue is 14.9%.

The TGA, DTG, DTA and exhaust gas mass spectroscopy for PAAc in air are found in Fig. 3. These data are summarized in Table 3, in which the behaviour

Table 3
Summary of thermal analysis for PAAc in air

Stage	TGA and DTG			DTA peaks (°C)	DSC heat (J/g)
	Onset (°C)	DTG peak (°C)	Mass loss (%)		
1	70	100	1.7	–	–
2	132	302	27.6	235, endo	393
3	325	420	38.4	exo	–
4	448	519	31.1	507, exo	–
Total			98.8		

of PAAc when heated in air is divided into four main stages based on the DTA, DTG and MS peaks. The first stage (70–132 °C) is similar to that seen for pyrolysis in argon: the evaporation of physically absorbed water and the release of moieties based on aromatic ions (m/z = 51, m/z = 78) above the glass transition temperature of 128 °C. In the second stage (132–325 °C), anhydride formation and decarboxylation become significant and moieties with m/z = 38 and m/z = 42 are released. The FTIR band related to unsaturated groups is more prominent in the PAAc exposed to 240 °C in argon than in the PAAc exposed to 240 °C in air.

The most significant difference between the thermal degradation in argon and in air is the large exotherm (DTA) representing polymer combustive oxidation in air for which there is no corresponding exotherm in argon. This exothermic oxidation yields a residual mass of 1.2% in air compared to 14.9% in argon. The exotherm begins during the third stage (325–448 °C) and is accompanied by the release of H_2O, CO_2, acrylic acid from depolymerisation, acetone species, species with m/z = 55 and new species with m/z = 91 and m/z = 106 from scission in the polymer and in the anhydride structures. The FTIR spectrum for PAAc exposed to 340 °C in air is similar to that for PAAc exposed to 340 °C in argon (Fig. 1). However, the band at 1810 cm^{-1}, related to the formation of glutaric anhydride, is seen for exposure in argon but not for exposure in air. During the fourth stage (from 448 °C), only H_2O and CO_2 are released and the residual mass reaches 1.2%, indicating complete oxidation.

In summary, the PAAc degradation mechanism includes dehydration, the formation of anhydride-type structures and their decarboxylation, chain scission and depolymerisation. Up to about 340 °C, there is no considerable difference between the pyrolysis of PAAc in argon or in air. Above 340 °C, pyrolysis in air yields thermo-oxidation and complete decomposition while pyrolysis in argon yields a carbonaceous residue.

3.3. Degradation of PAAc/Cu–N

The FTIR spectrum for as-cast 2/1 (Fig. 4a) is dominated by the band at 1385 cm^{-1} that is associated with the nitrate ion [23]. The FTIR absorption band at 1640 cm^{-1} is not seen for neat PAAc. This band is attributed to COO^- stretching (Table 1) and indicates the formation of a complex between the PAAc carboxylic groups and the copper ions. There may be two metal ion species present: metal ions bound to the polymer via two carboxylic anions and metal ions coordinated with H_2O at one site and bound to a carboxylic anion at the other [14]. The shift in the C–O stretching bands, from 1150 and 1240 cm^{-1} for PAAc to 1169 and 1247 cm^{-1} for 2/1, also indicates the formation of a copper–carboxylic complex [27]. In

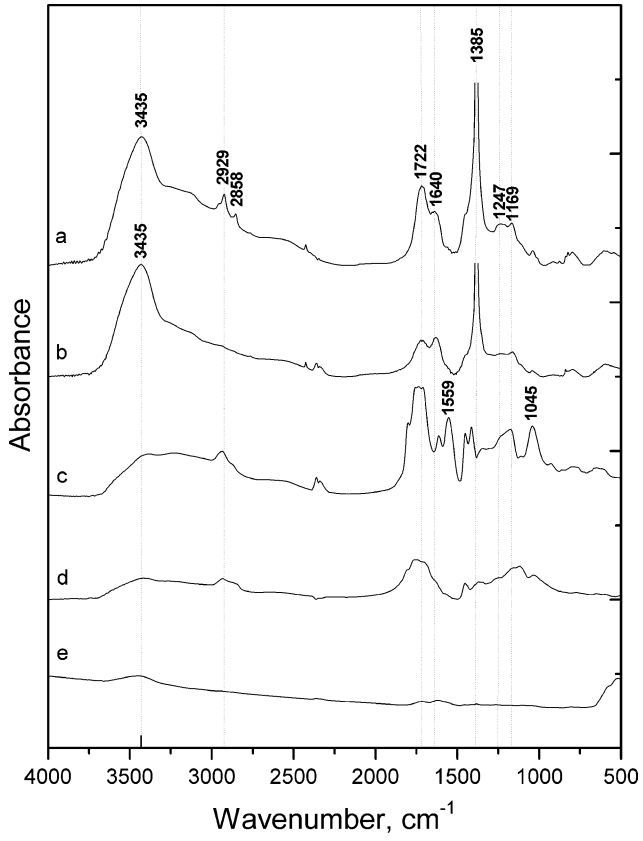

Fig. 4. FTIR spectra of 2/1 after exposure to high temperatures. (a) as cast; (b) 130 °C in argon; (c) 240 °C in argon; (d) 340 °C in argon; (e) 340 °C in air.

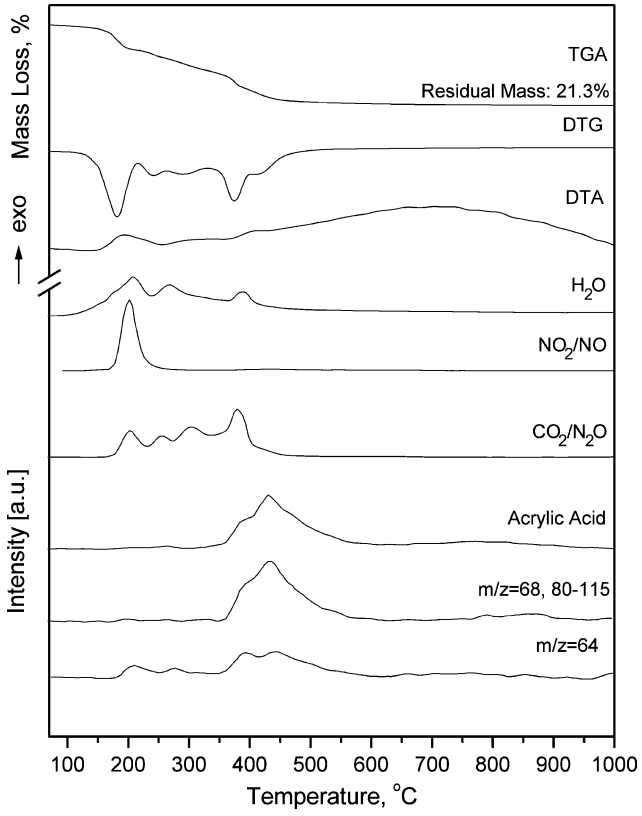

Fig. 5. Thermal analysis and exhaust mass spectra for 2/1 in argon.

addition, the C=O stretching peak has shifted from 1709 cm^{-1} for PAAc to 1722 cm^{-1} for 2/1. The presence of this band indicates that not all the carboxylic groups have formed complexes with copper [14,16,28].

The TGA, DTG, DTA and exhaust gas mass spectroscopy for 2/1 in argon are found in Fig. 5. These data are summarized in Table 4, in which the behaviour of 2/1 when heated in argon is divided into five main stages based on the DTA, DTG and MS peaks. As seen for PAAc, the first stage (70–103 °C) is associated with the evaporation of physically absorbed water. The second stage (103–216 °C) exhibits a mass loss of 24%, as water, nitrogen oxides and CO_2 are released during anhydride formation, anhydride decarboxylation and nitrate decomposition. The endothermic DSC peak for 2/1 at 158 °C (Fig. 6) represents the melting of residual crystallohydrate and nitrate decomposition. The exothermic peak at 180 °C represents the oxidative degradation of the polymer catalysed by the copper ion and advanced by the presence of nitrogen oxide species. The sizes of the endothermic peak and the exothermic peak increase with Cu–N content (Fig. 6) indicating their origin in the presence of Cu–N. The FTIR spectrum of 2/1 exposed to 130 °C in argon (Fig. 4) reveals a decrease in the relative intensity of the C=O band at 1722 cm^{-1} and a decrease in the relative intensity of the O–H band at 3435 cm^{-1}. These changes reflect the evaporation of physically absorbed water and the formation of anhydrides.

During the third stage (216–263 °C), water, nitrogen oxides and CO_2 continue to be released as anhydride formation, anhydride decarboxylation and nitrate decomposition continue. The FTIR band at 1385 cm^{-1} representing NO_3^- disappears after exposure to 240 °C, indicating that the nitrate groups have reacted. 2/1 exposed to 240 °C in argon (Fig. 4c) exhibits FTIR bands associated with glutaric and isobutyric anhydrides (1802, 1760 and 1740 cm^{-1}) [20] as well as the band

Table 4
Summary of thermal analysis for 2/1 in argon

Stage	TGA and DTG			DTA peaks (°C)	DSC heat (J/g)
	Onset (°C)	DTG peak (°C)	Mass loss (%)		
1	70	–	0.4	–	–
2a	–	–	–	158, endo	–
2b	103	182	24.0	180, exo	71
3	216	243	8.0	247, endo	–
4	263	292	12.1	–	–
5	331	375	34.2	383, exo	–
Total			78.7		

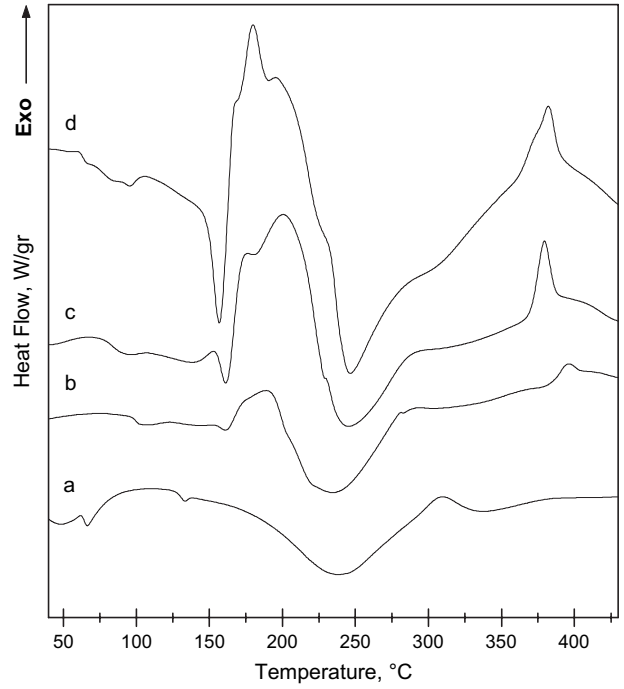

Fig. 6. DSC thermograms for PAAc/Cu–N in argon. (a) PAAc; (b) 10/1; (c) 4/1; (d) 2/1.

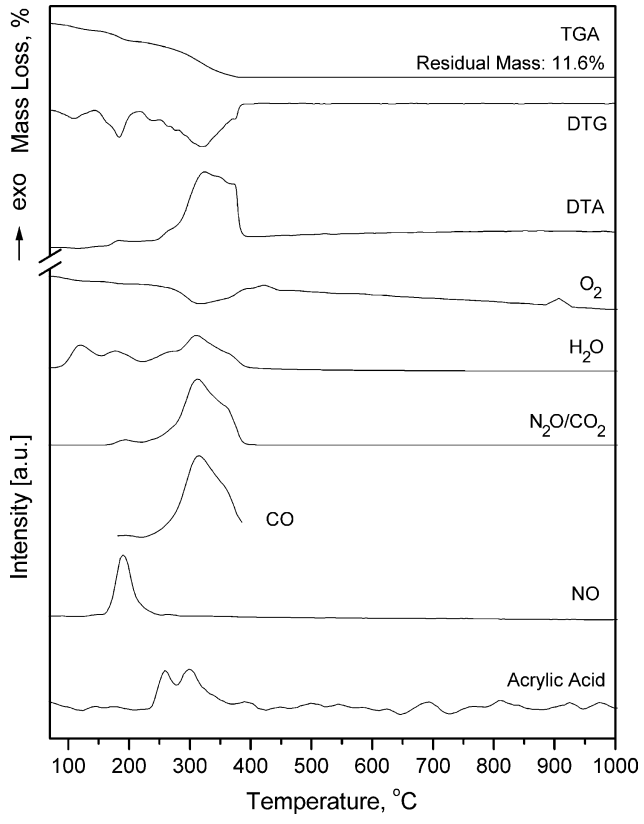

Fig. 7. Thermal analysis and exhaust mass spectra for 2/1 in air.

Table 5
Summary of thermal analysis for 2/1 in air

Stage	TGA and DTG			DTA peaks (°C)	DSC heat (J/g)
	Onset (°C)	DTG peak (°C)	Mass loss (%)		
1	70	109	12.4	–	–
2	143	184	18.4	159, endo	78
3	219	240	5.8	–	–
4	250	319	51.8	323, exo	10,000
Total			88.4		

associated with carboxylic groups (1708 cm^{-1}). The band at 1045 cm^{-1} indicates the presence of non-conjugated cyclic anhydrides. The band at 1615 cm^{-1} and the CH_2 scissors deformation at 1414 cm^{-1} are associated with unsaturation [23]. The relative intensity of the band associated with the C–O–H in-plane deformation at 1450 cm^{-1} is reduced, indicating a considerable decrease in carboxylic groups. The absorption at 1175 cm^{-1} most likely indicates the formation of cyclic ketones from the degradation of the carboxylic groups [24].

During the fourth stage (263–331 °C), only water and CO_2 are released, indicating the end of copper nitrate decomposition. During the fifth stage (331–550 °C) acrylic acid and low molecular weight compounds (m/z = 64, 68, 80–115) are released, indicating unzipping of the polymer chain. The exothermic peak at about 383 °C in the DSC thermograms in Fig. 6 represents CuO formation [14,18,19]. Assuming that PAAc in argon yields a residual mass of 14.9% and that the pyrolysis of Cu–N yields CuO, a residual mass of 21.7% can be predicted. The residual mass of 21.3% at 550 °C is very close to the prediction based on the pyrolysis of the individual components, indicating that the mechanisms of degradation for 2/1 in argon are similar to those of the components.

The TGA, DTG, DTA and exhaust gas mass spectroscopy for 2/1 in air are found in Fig. 7. These

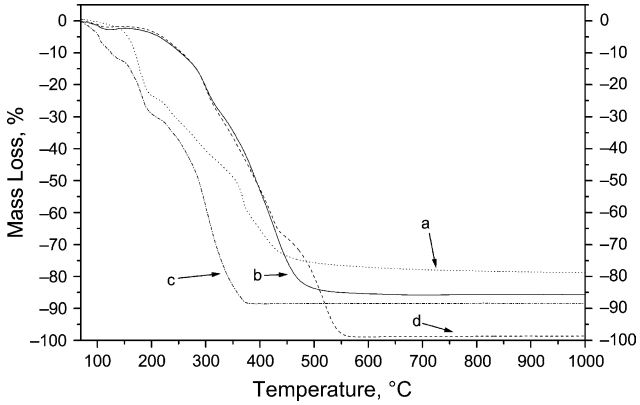

Fig. 8. TGA results for: (a) 2/1 in argon; (b) PAAc in argon; (c) 2/1 in air; (d) PAAc in air.

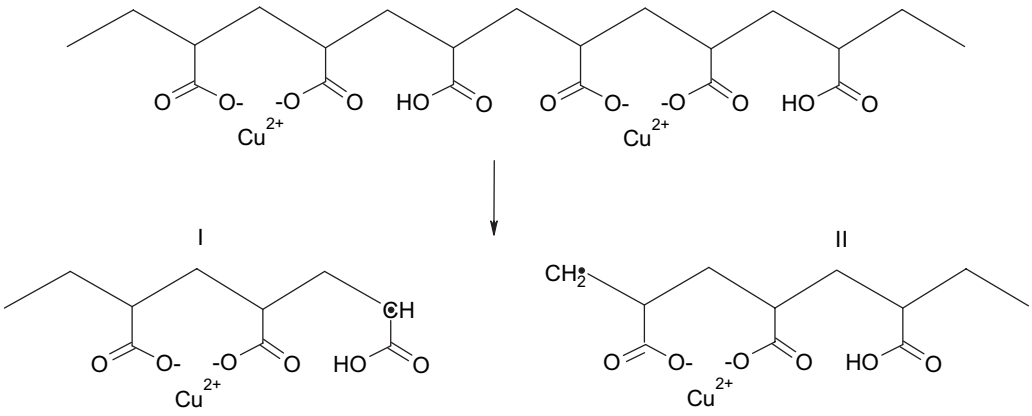

Scheme 1. Main chain scission.

data are summarized in Table 5, in which the behaviour of 2/1 when heated in air is divided into four main stages based on the DTA, DTG and MS peaks. The first stage (70–143 °C) exhibits a relatively high mass loss (12.4%). The reduction of the relative intensity of the carboxyl band at 1718 cm^{-1} for 2/1 exposed to 130 °C indicates anhydride formation. The second stage (143–219 °C) involves decomposition of the nitrate. In general, in the first three stages, up to 240 °C, there are no significant differences between decomposition in argon and in air.

In the fourth stage (above 250 °C) there is a large exothermic peak at 323 °C (10 kJ/g) reflecting thermo-oxidative degradation of organic matter. The exotherm is accompanied by the release of water, CO_2, CO, and a decrease in the oxygen level that indicates that oxygen is being rapidly consumed in the pyrolysis. The release of acrylic acid, indicating unzipping, continues until 380 °C (Fig. 7). After exposure of 2/1 to 340 °C in air, there are barely any traces of organic molecules in the FTIR spectrum (Fig. 4e). Assuming that PAAc in air decomposes completely and that the pyrolysis of Cu–N yields CuO, a residual mass of 11.7% can be predicted. The residual mass of 11.6% at 380 °C indicates that these assumptions are correct.

In summary, adding Cu–N to PAAc dramatically reduces the thermal stability. The degradation temperature for 2/1 is significantly lower than that of PAAc (Fig. 8). PAAc reaches a constant residual mass at 1000 °C in argon and at 580 °C in air, while 2/1 reaches a constant residual mass at 550 °C in argon and 380 °C in air.

These results indicate that the degradation mechanism for PAAc/Cu–N is similar to the one suggested by McNeill and Sadeghi [18,19]. Main chain scission leads to terminal macroradicals (Scheme 1) that can then react

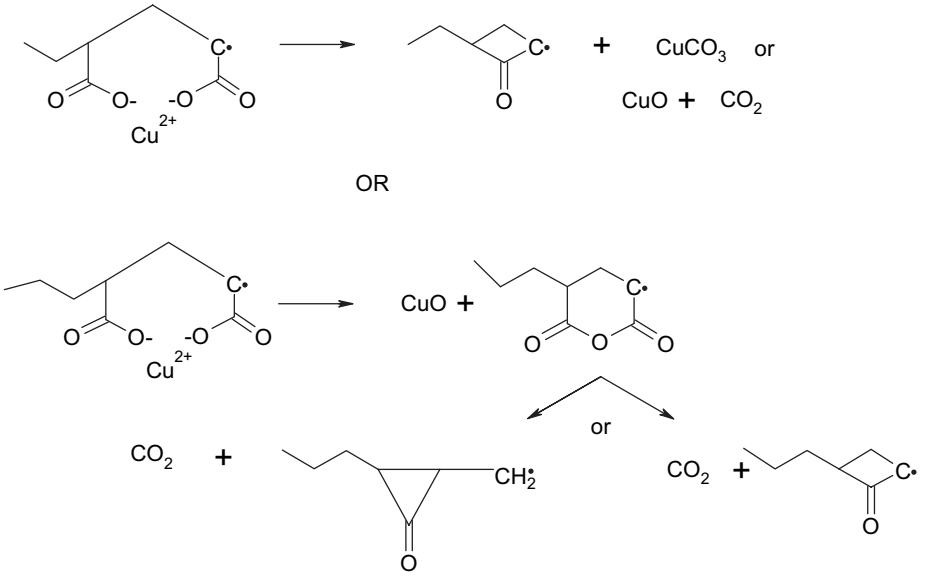

Scheme 2. Formation of copper carbonate and copper oxide.

by intramolecular transfer to give dimers, trimers and even acrylic acid. When backbone scission occurs, it will almost invariably be followed by side group scission and yield either a metal carbonate or a metal oxide. This mechanism also indicates that a number of low molecular weight organic compounds will be formed. Two intermediate terminal ring structures, formed as a result of side chain scission, may yield copper carbonate and copper oxide (Scheme 2).

4. Conclusions

The degradation of PAAc/Cu–N is a complex multistage process that is not always directly related to the degradation of the individual components. Adding Cu–N to PAAc causes a dramatic decrease in thermal stability. While the degradation of PAAc in argon yields a carbonaceous residue, no such residue was found for the degradation of PAAc/Cu–N in argon. The rate of PAAc/Cu–N degradation is significantly higher in air than in argon. The decomposition mechanisms include polymer chain scission, catalysed by copper ions, followed by the formation of the terminal macroradicals that generate low molecular weight organic compounds.

Acknowledgements

The authors gratefully acknowledge Dr. Irene von Lampe with thanks for her most helpful suggestions. The partial support of the German Israel Foundation and the Pozanski Fund are gratefully acknowledged.

References

[1] von Lampe I, Schultze D, Zygalsky F, Silverstein MS. Polym Degrad Stab 2003;81:57.
[2] Chien JCW, Gong BM, Madsen JM, Hallock RB. Phys Rev 1988; 38B:11853.
[3] von Lampe I, Bruckner A, Gotze S. Angew Macromol Chem 1997;25:157.
[4] von Lampe I, Schmalstieg A, Gotze S, Muller JP, Zygalsky F, Lorkowski HJ, et al. J Mater Sci Lett 1997;16:16.
[5] Zygalsky F, von Lampe I, Gotze S. Appl Supercond 1998; 6(10–12):795.
[6] von Lampe I, Schultze D, Zygalsky F. Polym Degrad Stab 2001; 73:87.
[7] von Lampe I, Gotze S, Zygalsky F. J Low Temp Phys 1996;105: 1289.
[8] Lumelsky Y. MSc thesis. Department of Materials Engineering, Technion, Haifa, Israel.
[9] Naka K, Tachiyama V, Ohki A, Maeda S. J Polym Sci Part A Polym Chem 1996;34:1003.
[10] Silverstein MS, Najary Y, Lumelski Y, von Lampe I, Grader GS, Shter GE. Polymer 2004;45(3):937.
[11] Pomogailo AD, Savost'ynov VS, Dzardimalieva GI, Dubovitskii AV, Ponomaryev AN. Izv Akad Nauk Ser Khim 1995;6:1096.
[12] von Lampe I, Zygalsky F, Hinrichsen G. Physica C 2000;341: 2381.
[13] Silverstein MS, Najary Y, Grader GS, Shter GE. J Polym Sci Part B Polym Phys 2004;42(6):1023.
[14] Skupinska J, Wilczura H, Boniuk H. Pol J Therm Anal 1986; 31(5):1017.
[15] McCluskey PH, Fishman GS, Snyder RL. J Therm Anal 1988; 34:1441.
[16] Allan JR, Bonner JG, Gerrard DL, Birnie J. Thermochim Acta 1991;185(2):295.
[17] Gronowski A, Wojtzak Z. J Therm Anal 1983;26:233.
[18] McNeill IC, Sadeghi SMT. Polym Degrad Stab 1990;30:213.
[19] McNeill IC, Sadeghi SMT. Polym Degrad Stab 1990;30:267.
[20] Cseri T, Bekassy S, Kenessey G, Liptay G, Figueras F. Thermochim Acta 1996;288(1–2):137.
[21] Jolly WL. The inorganic chemistry of nitrogen. New York: W.A. Benjamin; 1964. p. 69–88.
[22] Zivkovic ZD, Zivkovic DT, Grujicic DB. J Therm Anal Calorim 1998;53(2):617.
[23] Colthup NB, Daly LH. Introduction to infrared and Raman spectroscopy. 3rd ed. New York: Academic Press; 1990.
[24] McGaugh MC, Kottle S. J Polym Sci Polym Lett Ed 1967; 5(9):817.
[25] McNeill IC, Sadeghi SMT. Polym Degrad Stab 1990;29(2):233.
[26] Grant DH, Grassie N. Polymer 1960;1:125.
[27] Cardenas G, Munoz C, Carbacho H. Eur Polym J 2000;36(6): 1091.
[28] Allan JR, McCloy B, Gardner AR. Thermochim Acta 1993; 214(2):249.